RSC Advances

ROYAL SOCIETY OF CHEMISTRY

www.rsc.org/advances

Journal Name

RSCPublishing

ARTICLE

Tribological study of hydrolytically stable S-containing alkyl phenylboric esters as lubricant additives

Cite this: DOI: 10.1039/xoxxoooooox

Received ooth January 2012,
Accepted ooth January 2012

DOI: 10.1039/xoxxoooooox

www.rsc.org/

Zhipeng Li[a,b], Yilin Li[c], Yawen Zhang[a], Tianhui Ren [a,*],Yidong Zhao[d]

Three novel S-containing alkyl phenylboric esters, DSPB, TSPB and TBPB, were prepared and characterized. Compared with common boric esters, these three additives exhibit significant hydrolytic stability, which can be attributed to their specific molecular structures with the phenyl group conjugating with the electron-deficient boron that helps improving the hydrolytic stability of boric esters. The tribological properties were evaluated on a four ball tester, which suggest that all the synthesized additives act as anti-wear additives and have relatively high load-carrying capacities. Especially, it should be noted that DSPB exhibits both anti-wear and friction-reducing properties among the synthesized compounds. Furthermore, the worn surface was investigated by X-ray absorption near edge structure spectroscopy (XANES). The results demonstrate that the resulting tribofilm consists of trigonal and tetragonal coordination boron, iron sulfide and disulfide, and iron sulfate. Meanwhile, atomic force microscopy (AFM) was used to obtain the morphology of the tribofilm and the large pads elongated and orientated in the sliding direction have been found, which contribute to the anti-wear (AW) and extreme pressure (EP) performances.

1. Introduction

It is well known that base oil do not satisfy all the stringent requirements imposed on lubricants for use in heavy-duty machineries such as modern engines, hydraulic devices and large construction vehicles, which usually exhibit significant heat releasing and severe material consumption in their joint working parts. Such friction induced heat releasing and wear induced material consumption response for about one-third of the world total energy consumption every year [1, 2]. Various compounds containing boron, sulfur, phosphorus, halogens, nitrogen or metals as active components have been used as lubricating additives for the base oil to minimize wear, control friction, and thus to improve working efficiency as well as prolong the lifetimes of these heavy-duty machines. Zinc dialkyldithiophosphates (ZDDPs) have been widely used as lubricant additives in many heavy-duty mechanical conditions [3, 4]. However, there rises significant environmental issue for using ZDDPs that they produce zinc ashes, large amount of sulfur and phosphorus compounds, which can cause air pollution by directly releasing these hazardous chemicals into the air or indirectly poisoning the emission-control catalysts and further blocking the filters in car exhaust system [5]. Therefore, it is urgent to develop environmentally friendly lubricating additives to substitute or reduce the use of environmentally hazardous ZDDPs [6].

Boron-containing additives have been reported to be promising alternatives for substituting ZDDPs due to their comparable mechanical lubricating properties as well as low environmental impact [7]. One of the typical boron-containing additives is organic boric esters, for their specific properties of oil solubility, low-toxicity and biodegradability as well as anti-oxidation [8, 9]. It has been studied that the formation of a thin layer of boric oxide (B_2O_3) on the metal surfaces under extreme pressure is responsible for its anti-wear properties [10, 11]. Kapadia and his co-workers have proposed that amorphous networks of boric oxide with mixed three- (BO_3-) and four-(BO_4-) connective polymer units are formed on metal surfaces upon dehydration of H_3BO_3 [12]. But it is still unclear enough and more effort need to be made to reveal the tribological behaviors of boron on the metal surface.

However, due to the electron-deficiency of boron atom, the boric esters are inclined to hydrolyze under ambient condition, forming the oil-insoluble and abrasive boric acid, which is considered as a major limitation for its further application [13-15]. A common method to improve the hydrolytic stability of boric esters is introducing electron-rich nitrogen atom in the molecular structure to coordinate with boron for its stabilization [7, 15]. Even so, the N-containing boric esters still exhibit relatively poor hydrolytic stabilities due to the weakness of coordination bond between boron and nitrogen. Therefore, it is necessary to develop a new strategy on a molecular

design level to improve the hydrolytic stabilities of boric esters. In this report, we proposed an effective way to improve the hydrolytic stability of boric esters by introducing the alkyl phenyl group directly conjugating to the electron-deficient boron. The synthesized boric esters exhibits improved hydrolytic stabilities due to the p-π conjugating effect between the phenyl group and boron atom, and the long alkyl chain acting as a hydrophobic group that prevents the nucleophilic attack of water for the hydrolysis. Moreover, S-containing borate esters have been extensively studied in lubricant oil [5, 13, 16, 17]. It has been confirmed that a synergistic effect on the formation of protective film between S and B will occur when the element sulfur is introduced into the molecular structures of organic boric ester [18]. Therefore, three novel S-containing alkyl phenylboric esters were developed as lubricant additives and their tribological properties were evaluated. The results indicate that they all exhibit excellent anti-wear and friction-reducing properties as well as relatively high extreme pressure (EP) properties. We also believed that their specific tribological properties come from the specific tribological chemistry that occurred during the lubricating process under heavy-duty conditions. We utilized atomic force microscopy (AFM) and X-ray absorption near edge structure spectroscopy (XANES) to characterize the tribological surface on both morphological level and composition level and thus to reveal the mechanism of the occurred tribological chemistry.

2. Experimental

2.1 Base oil properties and synthesis of additives

A common mineral oil, hydro-isomerized and dewaxed base oil (HVI WH150, purchased from PetroChina Lanzhou Lubricating Oil R&D Institute in Lanzhou, China), was used as base oil in the test without any further treatment. The physical properties of the HVIW H150 mineral oil were given in Table 1.

Table 1
Physical properties of the HVIW H150 mineral oil

Parameter	Value
Density (20 ºC, g/cm^3)	0.844
Kinematic viscosity (mm^2/s)	
40 ºC	29.95
100 ºC	5.512
Viscosity index	125
Chrominance, number	0
Pour point (ºC)	-30
Open flash point (ºC)	226
Neutralizing value (mg KOH/g)	0.01
Extrinsic feature	Transparence
Evaporation loss, Noack 250 ºC, 1h (%)	10.15

All chemicals (purchased from Shanghai Chemical Company, Shanghai, China) were reagent grade and used without further purification. The 4-dodecylphenylboric acid was prepared according to the reported procedures [19, 20].

The synthesized additives are bis (1-(butylthio) propan-2-yl) 4-dodecylphenylboronate (TBPB), bis (1-(dodecyl-thio) propan-2-yl) 4-dodecylphenylboronate (DSPB) and bis (t-(dodecyl-thio) propan-2-yl) 4-dodecylphenylboronate (TSPB). The synthetic routes are depicted in Fig. 1 and the related synthetic procedures are described as follow:

Stoichiometric n-butanethiol (18.04 g, 0.20 mol), 1,2-epoxypropane (11.62 g, 0.20 mol) and triethylamine (20.24g, 0.20 mol) as catalyst were dissolved in 150 mL of dichloromethane in a 250 mL round-bottom flask. The reaction mixture was stirred at room temperature overnight. The resulting reaction mixture was extracted with dichloromethane, acidified with dilute hydrochloric acid and washed with water 3 times. The combined organic phase was dried over anhydrous $MgSO_4$ and filtered. The solvent was removed under reduced pressure to afford 1-(butylthio) propan-2-ol (26.24 g, 0.18mol) in 89 % yield.

4-dodecylphenylboric acid (14.51 g, 0.05 mol), 1-(butylthio) propan-2-ol (14.83 g, 0.10 mol) and catalytic amount of strong acid resin (Amberlite 732) were dissolved in 150 mL of toluene in a 250 mL round-bottom flask attached with a Dean-Stark trap for water separation. The reaction mixture was refluxed for 6 h under nitrogen atmosphere. The resulting reaction mixture was filtered and rotary evaporated to remove the toluene under vacuum resulting in (27.25 g, 0.05mol) TBPB in 99 % yield. DSPB (or TSPB) can be prepared by the reaction of between n-dodecylmercaptan (or t-dodecylmercaptan) and 4-dodecylphenylboric acid using the similar procedure. All of the synthesized additives were characterized by infrared spectroscopy (IR), nuclear magnetic resonance (NMR) and elemental analysis. The results of the elemental analysis are listed separately here in Table 2 for the convenience of indicating the percentages of sulfur or boron, which are important parameters in later discussion.

Bis (1-(butylthio) propan-2-yl) 4-dodecylphenylboronate (TBPB). Molecular formula: $C_{32}H_{59}BO_2S_2$. IR (KBr) (cm^{-1}): 2957.46m (-CH_3); 2926.53s, 2855.96m (-CH_2-); 1609.05w (C=C); 1457.08m, 1377.10m (-CH_3); 1341.85s (-CH_2-); 1310.81s (B-O); 758.54m (phenyl ring); 702.51w (C-B); 652.76w (C-S). 1H-NMR (δ, ppm, $CDCl_3$): 7.69-7.09 (4H, phenyl ring), 2.72-2.34 (9H, alkyl chain), 1.58-1.22 (34H, alkyl chain), 0.93-0.80 (12H, alkyl chain).

Bis (1-(dodecyl-thio) propan-2-yl) 4-dodecylphenylboronate (DSPB). Molecular formula: $C_{48}H_{91}BO_2S_2$. IR (KBr) (cm^{-1}): 2953.72m (-CH_3); 2925.48s, 2854.45m (-CH_2-); 1609.35w (C=C); 1456.38m, 1377.10m (-CH_3); 1336.75s (-CH_2-); 1318.60s (B-O); 759.51m (phenyl ring); 701.27w (C-B); 652.43w (C-S). 1H-NMR (δ, ppm, $CDCl_3$): 7.69-7.09 (4H, phenyl ring), 2.73-2.35 (9H, alkyl chain), 1.59-1.48 (9H, alkyl chain), 1.33-1.25 (60H, alkyl chain), 0.89-0.86 (9H, alkyl chain).

Bis (t-(dodecyl-thio) propan-2-yl) 4-dodecylphenylboronate (TSPB). Molecular formula: $C_{48}H_{91}BO_2S_2$. IR (KBr) (cm^{-1}): 2959.62m (-CH_3); 2928.79s, 2872.61m (-CH_2-); 1609.21w (C=C); 1460.11m, 1375.26m (-CH_3); 1342.51s (-CH_2-); 1319.25s (B-O); 759.51m (phenyl ring); 701.27w (C-B); 652.43w (C-S). 1H-NMR (δ, ppm, $CDCl_3$): 8.15-7.11 (4H, phenyl ring), 2.70-2.34 (7H, alkyl ring), 1.53-1.21 (50H, alkyl chain), 0.87-0.83 (30H, alkyl chain).

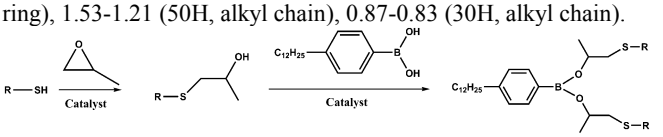

TBPB(R=*n*-C_4H_9); DSPB(R=*n*-$C_{12}H_{25}$); TSPB(R=*t*-$C_{12}H_{25}$)

Fig. 1 Synthesis of S-containing alkyl phenylboric esters

Table 2
Elemental analysis result of synthesized additives

Items	C (wt. %)	H (wt. %)	S(wt. %)	B(wt. %)
TBPB	69.37 (69.79)[a]	10.89 (10.80)[a]	11.66 (11.64)[a]	1.83 (1.96)[a]
DSPB	74.08 (74.37)[a]	11.99 (11.83)[a]	7.72 (8.27)[a]	1.36 (1.39)[a]
TSPB	74.04 (74.37)[a]	11.85 (11.83)[a]	7.90 (8.27)[a]	1.29 (1.39)[a]

[a] Calculated value (Balanced by oxygen)

2.2 Tribological evaluation

The tribological properties of TBPB, DSPB and TSPB as additives in mineral oil were investigated using a MMW-1 four-ball tester (manufactured by Ji'nan instrument manufacturer, China). The testing steel balls used in tribological measurement are 12.7 mm in diameter and made of GCr 15 bearing steel with 59–61 hardness of HRC. General tribological tests were conducted in ambient condition with rotating speed of 1450 rpm in duration of 30 min [5]. The coefficient of friction (COF) were recorded automatically by a computer linked to the four-ball tester and the values of wear scar diameter (WSD) on the three lower balls were measured using an optical microscope with an accuracy of ±0.01 mm. The maximum non-seizure loads (P_B values) tests of all additives were conducted according to Chinese national standard GB12583-98 which is similar to ASTM D-2783.

2.3 Hydrolytic stability test

A method of wet heating treatment that causes accelerated hydrolysis was used in hydrolytically stable test. Generally, 150 g of each lubricant sample (0.50 wt. % or 2.0 wt. % of each additive in the base oil) in a 200 mL beaker was placed in a hot and humid oven (50±2 ºC, relative humidity > 95 %). Each lubricant sample was monitored hourly until there was precipitation or no longer transparent which indicated the hydrolysis of the additive. The final time was recorded as a parameter for describing hydrolytic stability of each additives [21].

2.4 Surface analysis

A NanoScope IIIa atomic force microscope (Digital Instruments) was used to investigate the morphology of the tribo-surface on the testing steel balls. The surface roughness (root mean square, S_q) of anti-wear films was calculated by Image Analysis 2 software.

XANES data were collected at the Beijing Synchrotron Radiation Facility (BSRF), situated at the 2.2 GeV storage ring, Beijing Electron Positron Collider (BEPC) [22]. The K-edge spectra of boron were recorded using the soft X-ray optics beamline in the total electron yield (TEY) modes with the resolution of 1000 (E/ΔE). This beamline is monochromatized by a Monk-Gillieson monochromator, using an 800 mm^{-1} grating to cover the region of 190-210 eV. The K-edge spectra of sulfur were obtained using mid-energy spectroscopy beamline in the fluorescence yield (FY) modes with the double-crystal monochromator covering the energy of 2450-2500 eV. Both the K-edge of boron and sulfur provide chemical information on the surface of the reaction film. The thermal films were prepared under the following parameters: steel-ball, additive concentration 2.0 wt. %, temperature 150 ºC, time 6 h. While the tribofilms for XANES evaluation were generated from the tribological tests (the upper balls). All the ready-to-be-studied samples were gently rinsed in petroleum ether prior to XANES analyses [22]. Some model compounds were also scanned and recorded for the purpose of identification and comparison.

3. Results and discussion

3.1 Hydrolytic stabilities of synthesized additives

The hydrolytic stabilities of TBPB, DSPB and TSPB are listed in Table 3, Additives TB (tributyl borate) and NBO (N-containing borate ester) [23] are also listed in Table 3 for comparison. Overall, the hydrolytic stability of each additive decreases with the increase of the concentration, which ascribes to the high reaction probability between the additive molecule and water when the additive concentration is high. As is shown in Table 3, 0.5 wt. % and 2.0 wt. % of TB solutions start to hydrolyze in a very short time for 10 h and 2 h, respectively, while NBO exhibits better hydrolytic stability than TB due to the stabilized boron atom by the nitrogen coordination in its molecular structure [23]. For the synthesized compounds, their hydrolytic stabilities are considerably improved compared with TB and NBO, which can be attributed to two major points. One is the improved stability of boron by the phenyl group through p-π conjugation. Another is due to the existence of the long alkyl chain that prevents the nucleophilic attack of water, which is supported by the experimental observation that TSPB is more hydrolytically stable than DSPB and TBPB because its alkyl chain are longer (12C) than that of TBPB (4C) and more complicated (t-dodecyl) than that of DSPB (n-dodecyl). Therefore, the order of hydrolytic stabilities of the synthesized additives is TSPB > DSPB > TBPB. The observed experimental results and the trend of hydrolytic stabilities related to the molecular structures of the additives supported our rationale on molecular design. In addition, compared with a reported phenylboric ester [21], the synthesized additives also show better hydrolytic stabilities due to the hydrophobic activity of the long alkyl chain that prevents the nucleophilic attack of water to the boron atom.

Table 3
The hydrolytic stability of boric esters.

	0.5 wt. %	2.0 wt. %
TB	10 h	2 h
NBO	48 h	16 h
TBPB	312 h	89 h
DSPB	475 h	282 h
TSPB	599 h	496 h

3.2 Anti-wear (AW) performance

Figure 2 depicts the relationship between additive concentration and the wear scar diameter (WSD) of each additive in base oil under 294 N. It is obvious that all of the three additives are efficient to improve the anti-wear property of the base oil in tested concentration. The anti-wear performance of DSPB is the best of all while TBPB and TSPB are similar to each other. For DSPB it can be seen that the WSD firstly decreases sharply when the additive is added to the base oil, and with the increasing of additive concentration, the decline trend of WSD becomes gently. As for TBPB and TSPB, the WSD also decreases rapidly when additives are added, then remains relatively stable with a slightly increasing trend. This phenomenon can be explained from two aspects: the adsorption of additive on the metal surface and the corrosive abrasion caused by the sulfur in the additive molecules [24, 25]. TSPB contains branched chain structure, which makes its poor adsorption on the metal surface, while DSPB with more hydrophobic dodecyl group than TBPB leads to higher solubility in base oil, resulting in more adsorption of DSPB on the metal surface; On the other hand, when the additive concentration is low, the corrosion of S element can be ignored, but with the increase in additive concentration, the corrosive abrasion becomes gradually serious and finally counteracts the generation of protective film resulting in a dynamic equilibrium of abrasion. Furthermore, the different anti-wear performance of the synthesized additives can be ascribed to the different structure of the additive molecule [26]. As for the TSPB, because the more active sulfur in the branched-chain *t*-dodecyl than that of DSPB [26] leads to more serious corrosive abrasion, which impacts the compactness of the protective film. While for TBPB, as the *n*-butyl chain is short, associating with the element analysis, the content of sulfur is relatively high which results in more corrosive abrasion compared with DSPB when additives are in the same concentration [7]. Therefore, the WSD of TSPB and TBPB is bigger than that of DSPB.

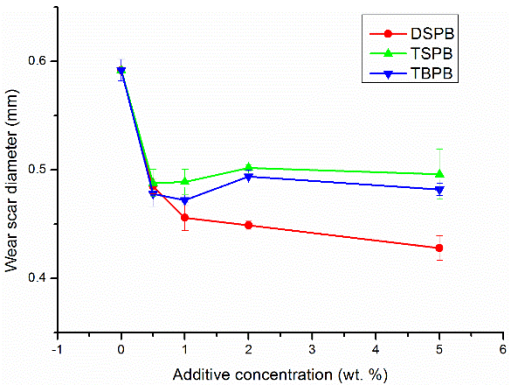

Fig. 2 The effect of the concentration of additives on wear scar diameter (applied load, 294 N; rotary speed, 1450 rpm; duration, 30 min).

3.3 Friction-reducing performance

The coefficient of friction (COF) of the synthesized compounds with different concentrations under the applied load of 294 N is exhibited in Fig. 3. It can be seen from the curves that the three compounds show different friction-reducing properties. For the performance of DSPB, the COF firstly increases when the additive concentration is low, then decreases with the increase of additive concentration, and finally stays relatively stable, which also suggests that the adsorbed additives interact with the freshly exposed worn surface on the friction pairs to form a protective adsorption film and/or reaction film. When the additive concentration is low, the protective film is not compact enough to resist the high shear force and could be damaged easily and the shear strength is high, resulting in the increase in COF [28]. With the increase of additive concentration from 0.5 wt. % to 2.0 wt. %, more additive molecules adsorb on the metal surface which leads to form a more compact protective film, and the adsorbed additive molecules act as adsorption film resulting in the decrease of shear strength, therefore the COF decreases. But when increasing the concentration continuously, the COF increases slowly, which means that the component of protective film transforms with the increasing of additive concentration. The detail will be discussed in the surface analysis of the tribofilm. For TBPB and TSPB, the COF does not change much compared with the COF of base oil, which means that the shear strength and roughness of the protective film keep relatively stable with the increase of additive concentration.

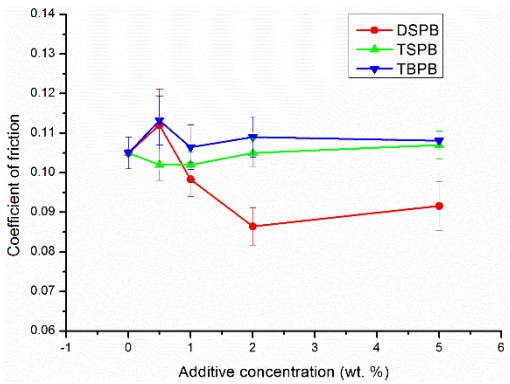

Fig. 3 The effect of the concentration of additives on friction coefficient (applied load, 294 N; rotary speed, 1450 rpm; duration, 30 min).

3.4 Extreme pressure (EP) performance

Effect of these S-containing long chain alkyl phenylboric esters under EP conditions is also investigated in this study. In general, the purpose of EP additives is to provide added wear protection and anti-seizing properties to both metallic surface and lubricant under higher loads and temperatures [26]. The maximum non-seizure loads (P_B values) of the base oil (HVIW H150), 2.0 wt. % DSPB, 2.0 wt. % TSPB and 2.0 wt. % TBPB in base oil are presented in figure 4. Significantly, all of the synthesized additives are effective in enhancing the P_B value of the base oil. It is also clear that TBPB is better than DSPB in increasing the P_B value, because according to the element analysis, the sulfur content in TBPB is higher than that of DSPB, leading to increase the maximum non-seizure load. TSPB is the best among the three additives in the EP performance. It has been studied that in the EP region, the surface layer is easily erased away and the fresh metal surface exposes continuously, therefore under this rigorous condition, additive exhibits best EP performance should be the one which reacts with the new formed metal surface to generate the most thickness protective film [29]. Therefore, TBPB exhibits better EP performance than that of DSPB due to its high content of sulfur. Meanwhile, the P_B value is also related to the reaction activity of sulfur. It is common that the activity of *t*-dodecylthio group is higher than that of *n*-dodecylthio group [27]. Upon the high shear force and tribo-heat generated from the EP condition, the C-S bond is cleavage and the *t*-dodecylthio group is more likely to react with the freshly exposed metal surface to form protective film, resulting in the improvement of maximum non-seizure load. However, though the reactivity of TSPB is higher than DSPB, the anti-wear property of TSPB does not perform better than that of DSPB, which is ascribed to the drawback of the branched group to access to the friction pairs. Therefore TSPB performs well in the short period property (P_B value), but express relatively poor performance in anti-wear property.

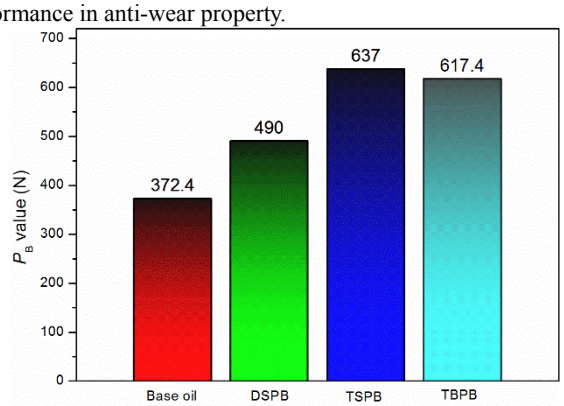

Fig. 4 Maximum non-seizure loads (P_B values) of the synthesized compounds (four-ball machine, rotation velocity of 1760 rpm for 10 s)

As discussed above, all of the three synthesized additives exhibit good anti-wear and relatively high EP properties, especially for the DSPB also shows friction-reducing performance. It makes us believe that there are tribological reaction occurring on the metal surface of the friction pairs under the boundary condition, thus to form a protective film covering the metal surface that prevents the direct metal-to-metal contacts between surface asperities. The different component and surface morphology of the protective film may be responsible for the different tribological performance. Therefore it is worth to investigate the nature of the protective film by surface analysis of the worn surface.

3.5 Surface analysis

3.5.1 Atomic force microscopy (AFM) analysis

AFM was used to examine the general morphology of the reaction films generated from the additives under AW conditions. The 2D and 3D AFM topography images of tribofilms generated from the synthesized additives are shown in Fig. 5 and Fig. 6. Comparison

with the 2D and 3D AFM images of tribofilms generated from the synthesized additives, it clearly reflects the tribofilms are quite heterogeneous. They are composed of large pads and are elongated and orientated in the sliding direction, which is several tens of microns long and several microns wide. This phenomenon is similar to the tribofilm lubricated with ZDDPs which had been reported previously [30-32]. The pads formed by DSPB are larger and more compactness than that of TSPB and TBPB, which explains that DSPB possesses better anti-wear property (Figure 2). The topography images also allow for accurate determination of the height profile of the anti-wear pads along with the topographic images taken from the dotted lines [32, 33] and the roughness of the metal surface of friction pairs [34]. A cross-sectional analysis of the pad was performed along the dotted line. The sectional analysis is shown in figure 5. From the figures the anti-wear pads of DSPB, TSPB and TBPB can be found to be 540.4 nm, 732.0 nm and 1048.0 nm thick, respectively. Associating with the EP properties presented in Fig. 4 and the 3D AFM topography images, it obviously indicates that the TSPB and TBPB are more active to react with the fresh metal surface to generate thicker protective films, which leads to better EP property. In spite of the thicker pad of TBPB, the more corrosive abrasion by sulfur resulting in a little worse in EP performance comparing with that of TSPB. Moreover, due to the corrosive abrasion, the compactness of the protective film is impacted which leads to smaller and more sparse pads, resulting in worse anti-wear property. The values of surface roughness (S_q) of DSPB, TSPB and DSPB are 145.3 nm, 163.1nm and 245.2 nm, respectively. This demonstrates that the smoother metal surface leads to the lower COF, corresponding to the data of friction-reducing performance shown in Fig. 3.

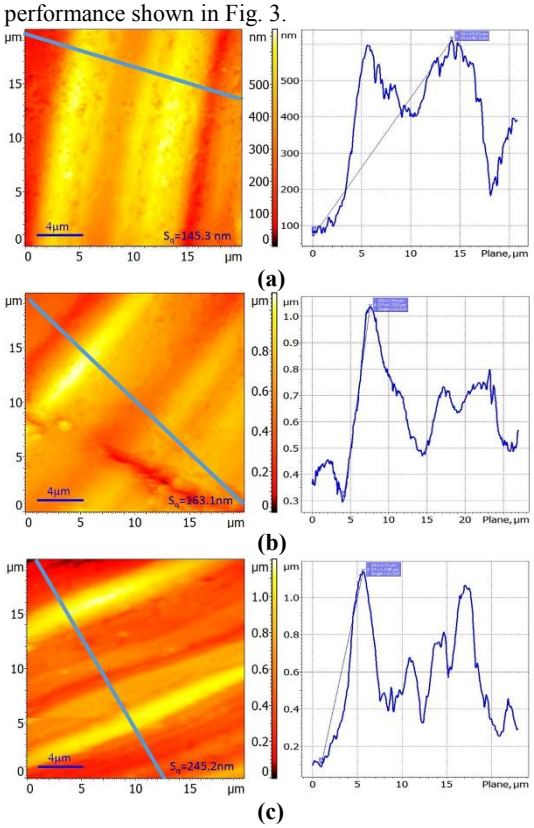

Fig. 5 AFM topography images (20×20 μm) of boundary films generated from the synthesized additives along with the topographic profiles images taken along the dotted lines: (a) DSPB; (b) TSPB; (c) TBPB (2.0 wt. % additive in base oil, applied load, 294 N; rotary speed, 1450 rpm; duration, 30 min)

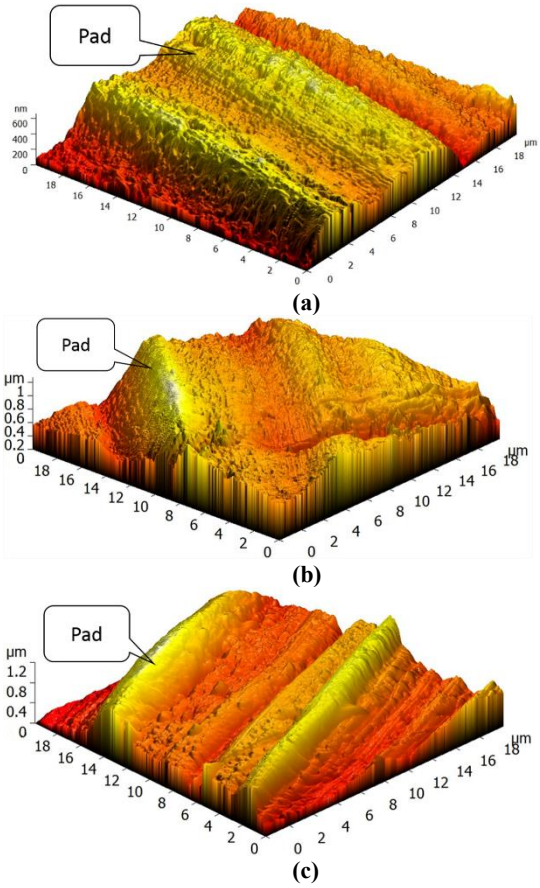

Fig. 6 3D topography images (20×20 μm) of boundary films generated from the synthesized additives: (a) DSPB; (b) TSPB; (c) TBPB (2.0 wt. % additive in base oil, applied load, 294 N; rotary speed, 1450 rpm; duration, 30 min)

3.5.2 XANES analysis of thermal film and tribofilm

From the AFM analysis of tribofilm, it obviously indicates that the formation of protective film by the synthesized additives. In order to obtain detail information of the chemical state of the protective film on the surface of the frictional pairs, X-ray absorption near edge structure (XANES) spectroscopy was used to investigate the thermal films and tribofilms generated from the synthesized additives in base oil. Several model compounds were also used for comparison to determine the chemical state of the film.

3.5.2.1 Thermal film

During the rubbing process, reactions between the adsorbed additives and friction pairs proceed with the help of tribo-heat, exoelectron, and catalytic effect of the renascent metal surface [35]. It is generally accepted that thermal films may provide further information about reactions taking place prior to friction and the temperature at the contact point between frictional pairs is about 150 ºC under moderate AW conditions [36]. Therefore the thermal films were prepared at the temperature of 150 ºC. The B K-edge (TEY) and S K-edge (FY) XANES spectra of the thermal films generated from synthesized additives at 2.0 wt. % along with some model compounds are presented in Fig. 7. Their peak positions along with some relevant model compounds are listed in Table 4 and Table 5. Comparing with the model compounds, it is obvious that the boron element in the synthesized additives has mainly transformed into trigonal and tetragonal coordination boron, while the sulfur element has mostly transformed into sulfate under the thermal oxidation condition. Especially for the DSPB, a small peak at 2473.7 eV which corresponds to alkyl sulfide [36], which suggests that the tribo-heat generated from the friction pairs plays an important role for the

formation the protective films. Moreover, iron sulfide or iron disulfide is not found in the thermal films. This can be attributed to the cover of iron oxide on the surface of the sample, preventing the active sulfur to react with the metal iron to form FeS or FeS_2 [22].

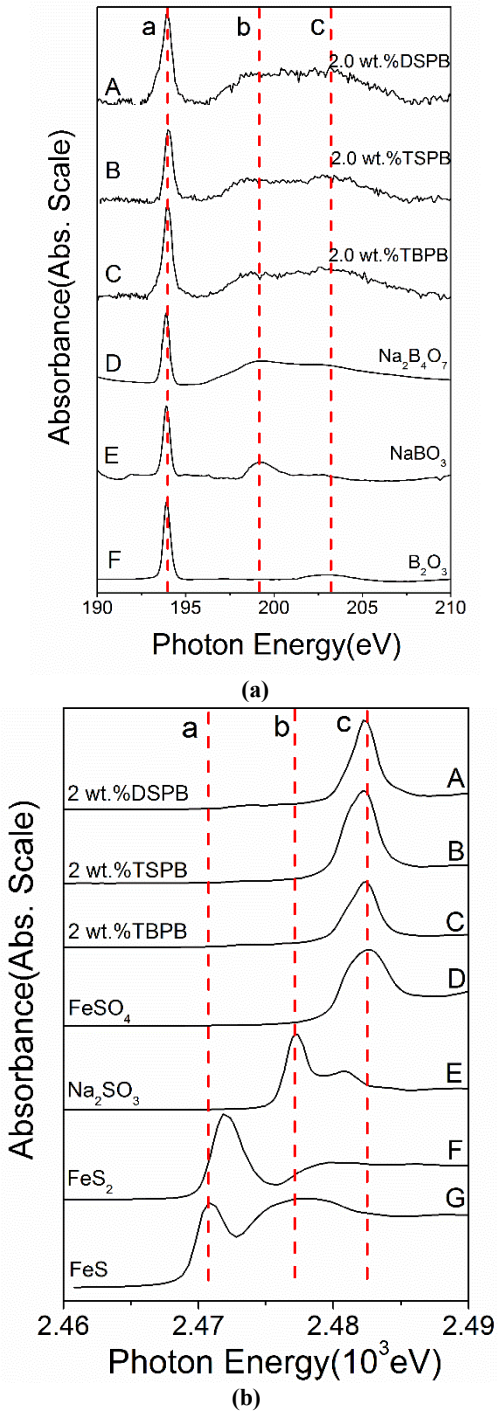

Fig. 7 XANES spectra of thermal films generated from synthesized additives along with some model compounds: a. B K-edge (TEY); b. S K-edge (FY)

Table 4 Peak positions of B K-edge (TEY) spectra of thermal films along with some model compounds.

	K-edge		
Samples	a	b	c
2.0 wt.% DSPB	193.9	199.2	203.2
2.0 wt.% TSPB	193.9	199.2	203.2
2.0 wt.% TBPB	193.9	199.2	203.2
Model compounds			
$Na_2B_4O_7$	193.9	199.2	203.2
$NaBO_3$	193.9	199.2	
B_2O_3	193.9		203.2

Table 5 Peak positions of S K-edge (FY) spectra of thermal films along with model compounds.

	K-edge				
Samples	a	b	c	d	e
2.0 wt.% DSPB			2473.7		2482.4
2.0 wt.% TSPB					2482.2
2.0 wt.% TBPB					2482.4
Model compounds					
FeS	2470.7			2477.2	
FeS_2		2472.0			
Na_2SO_3				2477.2	
$FeSO_4$					2482.4

3.5.2.2 Tribofilm

The B K-edge (TEY) and S K-edge (FY) XANES spectra of the tribofilms generated from synthesized additives at 0.5 wt. % and 2.0 wt. % along with some model compounds are presented in Fig. 8. Their peak positions along with some relevant model compounds are listed in Table 6 and Table 7.

As for the boron K-edge XANES spectra, it can be seen that the curves of tribofilms generated from the synthesized compounds are similar to that of thermal films, and do not show much significant difference with the increasing of additive concentration except for the peak intensity. Same as the thermal film, the boron in additive has mainly transformed into trigonal and tetragonal coordination boron by the tribo-heat, which also demonstrates that the tribo-heat generated from the friction pairs plays an important role for the formation of protective films. The result is consistent with the previous reports [10, 11, 37]. Furthermore, it also can be found that the peak intensity increases gradually with the increase of additive concentration, which suggests that more adsorbed additive molecules react with the metal surface to generate thicker films. It is known that the boron oxide is very hard material [38], which accounts for the decline of WSD and increase of COF when the additive concentration is high. Since more hard materials generated, the protective film become more compact to prevent the direct metal surface contact leading to the decline of WSD, meanwhile the roughness of the surface increases, resulting in the increase in COF.

With regard to the sulfur K-edge XANES spectra, it is apparent that the film chemistry changes under the boundary condition of high shear force and tribo-heat generated from rubbing process, which can be explained that during the sliding process, the fresh metal surface was exposed continuously, therefore the active sulfur could react with the fresh metal surface [22]. There are three apparent peaks suited at 2470.7 eV, 2477.2 eV and 2482.4 eV, respectively. According to the spectra of model compounds, it can be found that the tribofilm is mainly composed of iron sulfide and iron sulfate. In addition, the peak at 2472.0 eV attributed to iron disulfide can also be found though it is not significant. For DSPB, it is obvious that the peak of sulfide and disulfide is weaker than that of TSPB while the peak of sulfate is stronger. Since the sulfide and disulfide films are easily worn down during rubbing processes, which leads to inferior anti-wear performance of TSPB [26]. Though the peak of sulfide and disulfide of TBPB is also weak (panel F), due to the corrosion caused by high content of sulfur, the anti-wear performance of TBPB is not as good as DSPB. This explains that the anti-wear

performance of DSPB is better than that of TSPB and TBPB.

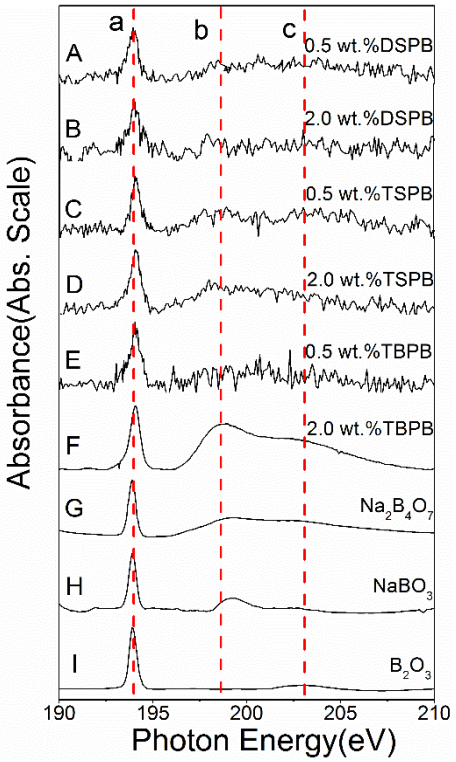

(a)

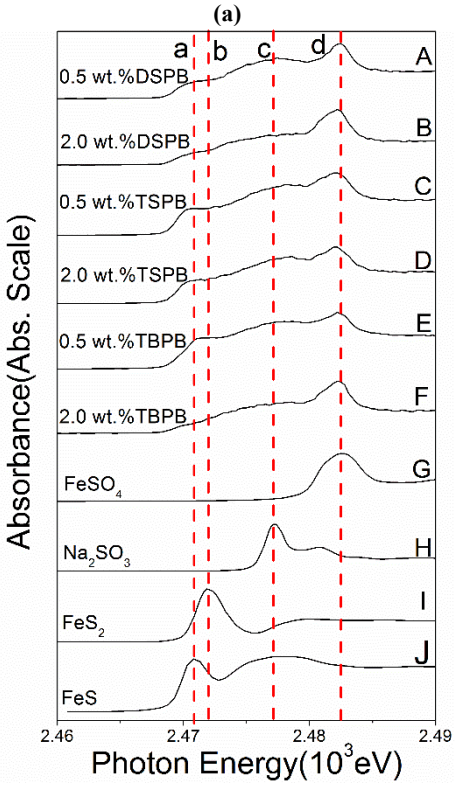

(b)

Fig. 8 XANES spectra of tribofilms generated from synthesized additives along with some model compounds: a. B K-edge (TEY); b. S K-edge (FY) (applied load, 294 N; rotary speed, 1450 rpm; duration, 30 min)

Table 6 Peak positions of B K-edge (TEY) spectra of thermal films along with some model compounds.

	K-edge		
Samples	a	b	c
0.5 wt.% DSPB	193.9	199.2	203.2
2.0 wt.% DSPB	193.9	199.2	203.2
0.5 wt.% TSPB	193.9	199.2	203.2
2.0 wt.% TSPB	193.9	199.2	203.2
0.5 wt.% TBPB	193.9	199.2	203.2
2.0 wt.% TBPB	193.9	199.2	203.2
Model compounds			
$Na_2B_4O_7$	193.9	199.2	203.2
$NaBO_3$	193.9	199.2	
B_2O_3	193.9		203.2

Table 7 Peak positions of S K-edge (FY) spectra of thermal films along with model compounds.

	K-edge			
Samples	a	b	c	d
0.5 wt.% DSPB	2470.7	2472.0	2477.2	2482.4
2.0 wt.% DSPB	2470.7	2472.0	2477.2	2482.4
0.5 wt.% TSPB	2470.7	2472.0	2477.2	2482.4
2.0 wt.% TSPB	2470.7	2472.0	2477.2	2482.2
0.5 wt.% TBPB	2470.7	2472.0	2477.2	2482.4
2.0 wt.% TBPB	2470.7	2472.0	2477.2	2482.4
Model compounds				
FeS	2470.7		2477.2	
FeS_2		2472.0		
Na_2SO_3			2477.2	
$FeSO_4$				2482.4

3.6 Discussion

Base on the hydrolytic stable test, tribological evaluation and surface analysis by XANES and AFM, it can be inferred that under the boundary lubrication condition, a complicated tribofilm is generated from the synthesized additives, which prevents the direct contact of asperities on the surface of friction pairs. As for the hydrolytic stability, the directly linking long chain alkyl phenyl with boron is an efficient method to enhance the hydrolytic stability of borate ester. Meanwhile, the group structure around the boron element also imposes on the hydrolytic stability. The complicated group is beneficial for improving hydrolytic stability of borate ester. However, for the tribological properties, the amount and activity of sulfur have greatly influenced on the AW and EP performance. There is an equilibrium for the amount of sulfur containing in the molecule of additive because of the corrosive abrasion. With regard to the surface analysis of XANES and AFM, it can be found that the tribofilm consists large pads on the asperities of metal surface, composed of trigonal and tetragonal coordination boron, iron sulfide and disulfide, and iron sulfate. The compactness and roughness of the tribofilm correspond to the AW and friction-reducing properties. The more compact and smooth tribofilm result in better AW and friction-reducing performance.

4. Conclusions

The hydrolytic stability, tribological performance and wear behaviour of three S-containing alkyl phenylboric esters have been investigated and discussed. The results can be summarized as follows.

- The three synthesized compounds used as additive in base oil exhibit superiority in hydrolytic stability comparing with tributyl borate, NBO and phenylboric ester reported

previously, which demonstrates that the designed molecular structure, by introducing long chain alkylphenyl group to conjugate with the electron-deficient boron, is effective on enhancing the hydrolytic stability of borate ester, meanwhile, the group structure around the boron element also imposes on the hydrolytic stability.

- The synthesized compounds possess relatively good anti-wear performance as additive in base oil, especially for DSPB which also has friction-reducing property. Combined with the excellent hydrolytic stability, which makes DSPB a promising candidate for the future lubricant additives.
- The AFM analysis of tribofilm clearly demonstrates that the compactness and smooth of DSPB is better than that of TSPB and TBPB, which leads to the better AW and friction-reducing performance.
- The boron and sulfur K-edge XANES analysis reveal that the thermal film is mainly composed of trigonal and tetragonal coordination boron, and iron sulfate, while the tribofilm consists of trigonal and tetragonal coordination boron, iron sulfide and disulfide, and iron sulfate, moreover the tribo-heat is a key factor for the boron to generate tribofilm.

Acknowledgements

The authors are grateful to the National Natural Science Foundation of China (grant No. 21272157), the Beijing Synchrotron Radiation Facility (Grant No. SR06033) and the open projects of the Key State Lab of Solid Lubrication in Lanzhou of China (Grant No. 1205) for the financial support to the work reported here. We gratefully thank Beijing Synchrotron Radiation Facility for the XANES analysis.

Notes and references

[a]School of Chemistry and Chemical Engineering, Key Laboratory for Thin Film and Microfabrication of the Ministry of Education, Shanghai Jiao Tong University, 200240, China.
[b]Laboratory of Solid Lubrication, Lanzhou Institute of Chemical Physics, Chinese Academy of Sciences, Lanzhou 730000, China
[c]Voiland School of Chemical Engineering and Bioengineering, Washington State University, Pullman, WA 99164, USA;
[d]Beijing Synchrotron Radiation Facility, Institute of High Energy Physics, Chinese Academy of Sciences, Beijing 100039, China

*Corresponding author. Tel.: +86 21 5474 7118
E-mail address: thren@sjtu.edu.cn (TH. Ren).

1 W. J. Bartz, *Tribology International*, 2006, **39**, 728-733.
2 K. Holmberg, P. Andersson and A. Erdemir, *Tribology International*, 2012, **47**, 221-234.
3 F. U. Shah, S. Glavatskih, E. Hoglund, M. Lindberg and O. N. Antzutkin, *Acs Applied Materials & Interfaces*, 2011, **3**, 956-968.
4 N. J. Mosey, T. K. Woo, M. Kasrai, P. R. Norton, G. M. Bancroft and M. H. Muser, *Tribology Letters*, 2006, **24**, 105-114.
5 J. Li, X. Xu, Y. Wang and T. Ren, *Tribology International*, 2010, **43**, 1048-1053.
6 F. U. Shah, S. Glavatskih and O. N. Antzutkin, *Tribology Letters*, 2011, **45**, 67-78.
7 H. Spikes, *Lubrication Science*, 2008, **20**, 103-136.
8 B. A. Baldwin, *Wear*, 1977, **45**, 345-353.
9 R. Choudhary and P. Pande, *Lubrication Science*, 2002, **14**, 211-222.
10 A. Papay, *Lubrication Science*, 1998, **10**, 209-224.
11 D. Philippon, M. I. Barros-Bouchet, O. Lerasle, T. Mogne and J. M. Martin, *Tribology Letters*, 2010, **41**, 73-82.
12 R. Kapadia, R. Glyde and Y. Wu, *Tribology International*, 2007, **40**, 1667-1679.
13 G. Shen, Z. Zheng, Y. Wan , X. Xu, L. Cao, Q. Yue, T. Sun and A. Liu, *Wear*, 2000, **246**, 55-58.
14 Z. Zheng, G. Shen, Y. Wan, L. Cao, X. Xu, Q. Yue and T. Sun, *Wear*, 1998, **222**, 135-144.
15 F. U. Shah, S. Glavatskih and O. N. Antzutkin, *Tribology letters*, 2013, **51**, 281-301.
16 Y. Sun, L. Hu and Q. Xue, *Wear*, 2009, **266**, 917-924.
17 J. Zhang, W. Liu, and Q. Xue, *Wear*, 1999, **224**, 68-72.
18 Q. Gong, W. Liu and C. Ye, *Tribology*, 2002, **22**, 360-363.
19 M. A. Hall, J. Xi, C. Lor, S. Dai, R. Pearce, W. P. Dailey and R. G. Eckenhoff, *Journal of medicinal chemistry*, 2010, **53**, 5667-5675.
20 J. X. Cai, A. Farhat, P. B. Tsitovitch, V. Bodani, R. D. Toogood and R. S. Murphy, *Journal of Photochemistry and Photobiology a-Chemistry*, 2010, **212**, 176-182.
21 Y. Wang, J. Li, Z. He and T. Ren, *Proceedings of the Institution of Mechanical Engineers, Part J: Journal of Engineering Tribology*, 2008, **222**, 133-140.
22 J. Li, H. Ma, T. Ren, Y. Zhao, L. Zheng, C. Ma and Y. Han, *Applied Surface Science*, 2008, **254**, 7232-7236.
23 J. Yan, X. Bai, T. Ren and X. Zeng, *Petroleum Products Application Research*, 2012, **30**, 109-111.
24 J. W. You, F. F. Li and B. S. Chen, *China Petroleum Processing Petrochemical Technology*, 2010, **12**, 43-48.
25 H. Wu, J. Li, H. Ma and T. Ren, *Surface and Interface Analysis*, 2009, **41**, 151-156.
26 H. Chen, J. Yan, T. Ren, Y. Zhao and L. Zheng, *Tribology Letters*, 2012, **45**, 465-476.
27 D. Li, X. Yu and Y. Dong, *Applied Surface Science*, 2007, **253**, 4182-4187.
28 S. Aoki, A. Suzuki and M. Masuko, *Proceedings of the Institution of Mechanical Engineers, Part J: Journal of Engineering Tribology*, 2006, **220**, 343-351.
29 X. Zeng, J. Li, X. Wu, T. Ren and W. Liu, *Tribology International*, 2007, **40**, 560-566.
30 M. N. Najman, M. Kasrai and G. M. Bancroft, *Tribology Letters*, 2004, **17**, 217-229.
31 M. A. Nicholls, G. M. Bancroft, M. Kasrai, P. R. Norton, B. H. Frazer and G. De Stasio, *Tribology Letters*, 2005, **18**, 453-462.
32 M. A. Nicholls, G. M. Bancroft, P. R. Norton, M. Kasrai, G. De Stasio, B. H. Frazer and L. M. Wiese, *Tribology Letters*, 2004, **17**, 245-259.
33 B. Vengudusamy, A. Grafl, F. Novotny-Farkas, T. Schimmel and K. Adam, *Tribology International*, 2013, **67**, 199-210.
34 V. Jaiswal, R. B. Rastogi, R. Kumar, L. Singh and K. D. Mandal, *Journal of Materials Chemistry A*, 2014, **2**, 375.
35 C. McFadden, C. Soto and N. D. Spencer, *Tribology international*, 1997, **30**, 881-888.
36 M. N. Najman, M. Kasrai and G. M. Bancroft, *Tribology Letters*, 2003, **14**, 225-235.
37 J. Yan, X. Zeng, E. van der Heide and T. Ren, *Tribology International*, 2014, **71**, 149-157.
38 P. Ball, *Nature materials*, 2010, **9**, 6.

Graphic abstract

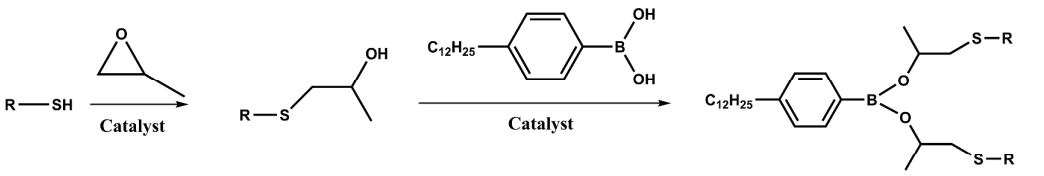

TBPB(R=*n*-C_4H_9); DSPB(R=*n*-$C_{12}H_{25}$); TSPB(R=*t*-$C_{12}H_{25}$)

S-containing alkyl phenylboric esters with excellent hydrolytic stability used as lubricant additives